



# Effect of Powder Preparation on the Microstructure and Wear of Plasma-Sprayed NiAl/CrB<sub>2</sub> Composite Coatings

Olena Poliarus<sup>1</sup> · Jerzy Morgiel<sup>2</sup> · Piotr Bobrowski<sup>2</sup> · Maciej Szlezynger<sup>2</sup> · Oleksandr Umanskyi<sup>1</sup> · Maxim Ukrainets<sup>3</sup> · Lukasz Maj<sup>2</sup> · Oleksiy Kostenko<sup>1</sup>

Submitted: 27 November 2018 / in revised form: 11 February 2019 / Published online: 30 April 2019  
© The Author(s) 2019

**Abstract** The properties of plasma-sprayed composite coatings depend to a large extent on the homogenization of the powders used for their deposition. In order to investigate this relation, mixtures of NiAl and CrB<sub>2</sub> (15 and 30 wt.%) powders were prepared via an organic binder (a), hot pressing (b) or sintering (c). The obtained composite agglomerates were sprayed on cylindrical AISI 310S steel pins. Their wear resistance was assessed through a pin-on-disc dry-sliding wear test carried out at 500 °C (a counterbody of NiAl coating was also deposited on AISI 310S). All the composite coatings presented strongly reduced the wear rate when compared with the reference NiAl coatings ( $9.8 \times 10^{-5} \text{ mm}^3/\text{Nm}$ ). Those with 30 wt.% CrB<sub>2</sub> addition and obtained via the (a), (b) and (c) routes had 3.8, 2.9 and  $1.4 \text{ mm}^3/\text{Nm} \cdot 10^{-5}$ , while those with 15 wt.% CrB<sub>2</sub> for the same routes had 2.6, 0.9 and  $0.7 \text{ mm}^3/\text{Nm} \cdot 10^{-5}$ , respectively. The least damage was present in the NiAl (15 wt.% CrB<sub>2</sub>) coating obtained using route (c), due to the microstructure refinement already achieved at the sintering stage and the good reactive binding of CrB<sub>2</sub> with the coating matrix, established during plasma spraying. Increasing the CrB<sub>2</sub> addition up to 30 wt.% promotes crack propagation accelerating wear.

**Keywords** microstructure · NiAl/CrB<sub>2</sub> · plasma-spray coatings · wear resistance

## Introduction

Atmospheric plasma sprayed coatings are applied to improve the wear and corrosion resistance of both mechanically and thermally-loaded machine parts. Coatings applied on gas turbine blades allow their working temperature range to be increased, which helps to raise turbine efficiency.

Intermetallic compounds, like NiAl, are very well known for their remarkable mechanical strength and oxidation resistance (Ref 1). However, their application as a high-temperature structural material is limited due to their susceptibility to plastic deformation at temperatures above 500 °C (Ref 1, 2). This eventually leads to the cracking, delamination and subsequent removal of a protective oxide film from the friction zone. As a consequence, this causes the repeated seizure of the contact surfaces, activating adhesive wear, which is the most destructive of damage mechanisms. One of the ways to improve the high-temperature wear resistance of NiAl could be achieved through its strengthening with refractory compounds, like borides (Ref 3-8).

The addition of refractory borides, like TiB<sub>2</sub>, ZrB<sub>2</sub> or CrB<sub>2</sub>, into a NiAl coating resulted in significant lowering of its wear at high temperatures (Ref 9-11). The last of these borides turned out to be especially effective in this role, as it allowed wear to be lowered by four times. The presence of boride particles helps to redistribute external loading within the matrix, and they are much faster oxidized when compared to the NiAl intermetallic. Repeated growth and removal of the oxide layer from boride

✉ Jerzy Morgiel  
j.morgiel@imim.pl

<sup>1</sup> Frantsevich Institute for Problems of Materials Science, National Academy of Sciences of Ukraine (IPMS NASU), 3 Krzhyzhanovsky St., 03142 Kiev, Ukraine

<sup>2</sup> Institute of Metallurgy and Materials Science, Polish Academy of Sciences, 25 Reymonta St., 30-059 Kraków, Poland

<sup>3</sup> Progresstech-Ukraine LCC, 3 Sholudenko St., 04116 Kiev, Ukraine

particles helps oxide debris to accumulate on working surfaces, acting as a solid lubricant. Its presence prevents seizure between the surfaces of the friction couple and changes the wear mechanism of the materials involved from adhesive to oxidative.

The properties of such composite coatings depend to a large extent on the procedure of their deposition, including the powder preparation stage. Observations of the worn surfaces of coatings obtained from initial NiAl and CrB<sub>2</sub> agglomerated powders stabilized with organic binders showed that the amount of refractory phase found in them is well below the nominal 15 wt.% (Ref 9). Evidently, at high temperatures developed during the atmospheric plasma spraying (APS), the organic binder connecting the powder particles is burnt-out at very early stages of the deposition process. Next, due to differences in size and weight between the intermetallic and boride particles, a significant fraction of the latter falls outside the jet center, never reaching the coating. Therefore, another method of composite powder preparation, excluding organic binders and enabling the loss of the refractory phase during the plasma spray deposition process to be avoided, should be sought.

The present work was aimed at elaborating alternative ways to those using an organic binder for the preparation of NiAl/CrB<sub>2</sub> composite powder agglomerates needed for atmospheric plasma-spraying deposition processes. Both hot pressing and vacuum sintering were tried in this role. Their effect on the microstructure of such plasma-sprayed composite coatings deposited on AISI 310S steel was investigated using both SEM and TEM methods, while the dry wear was assessed through tests performed at 500 °C. This temperature was decided on as it both marks the start of intensive plastic deformation of nickel aluminides and corresponds to routine compressor operating conditions.

## Experimental Techniques

The commercial powders of NiAl intermetallic (supplied by Polema JSC) and chromium boride (by Komplex) were used as base materials. Both powders were milled and sieved to the powder size 16–20 μm for the intermetallic and 5–7 μm for CrB<sub>2</sub>. The particle size distribution was measured by SK-Laser Micron Sizer PRO-7000 (Germany). Composite agglomerates of NiAl-15 and 30 wt.% CrB<sub>2</sub> for atmospheric plasma deposition processes were obtained by three different routes:

- using an organic binder (nitrocellulose, which is a component of Zapon lacquer);

- hot-pressed at  $T = 1450$  °C at a load of 10 MPa (heating rate of 100 °C/min without a protective atmosphere);
- vacuum-sintered at  $T = 1650$  °C for 30 min at  $10^{-3}$  Pa.

Briquettes obtained in the above ways were crushed and ground to 70–100 μm. Next, the resulting powders were deposited by the APS method on the top of cylindrical AISI 310S stainless steel rods (pins) of 10 mm height and 5 mm diameter. The coatings were deposited normally to the pin surfaces. The plasma-supporting gas was a mixture of argon and hydrogen and the carrier gas was argon. A Metco F4-MB (USA) plasma spray gun (maximum power, 50 kW) was used as a plasma generator for coating deposition. It was attached to UPU-3D (USSR) plasma spraying equipment modified in the Frantsevich Institute for Problems of Material Science. UPU-3D spraying equipment is a multipurpose one and combines a controller and power supply. Spraying was conducted in a 15VB (USSR) JAMBox. To improve the adhesion of the sprayed coatings to the steel substrate, an intermediate Ni<sub>3</sub>Al layer coating of 25- to 30-μm thickness (bond coat) was also deposited by the APS method (details in Table 1). The coating thickness after APS deposition in all cases was  $0.5 \pm 0.05$  mm.

The amount of CrB<sub>2</sub> was estimated using the secant method based on SEM images. According to this method, the average amount of the refractory phase was evaluated as the area of CrB<sub>2</sub> crystallites per 1 cm<sup>2</sup> (in five different areas of the surface coating). Up to 10 secant lines of 100 μm length, spaced by 10 μm, were drawn on the sample surface. The content of CrB<sub>2</sub> phase was calculated according to the formula:

$$dl = l/n$$

where  $n$  is the number of grains on a secant line, and  $l$  is the length of a secant line in μm.

As a counter-body, an AISI 310S stainless steel disc (radius, 20 mm) with a NiAl coating was used. The coating thickness was  $\sim 0.5$  mm, while its porosity was below 5%. A wear test was carried out with the rotating pin-on-disc scheme (track radius, 15 mm) using a CETR (presently Bruker) UMT-2 friction machine equipped with a high-temperature module, as presented in Fig. 1. The dry-sliding wear test conditions corresponded to those that take place during the operation of most gas turbine engines. Therefore, a tribo-pair was chosen, taking into account that the developed wear-resistant composite coating will be applied to the top of the gas turbine blade, while the NiAl forms the compressor housing. Similarly, the test temperature of  $\sim 500$  °C was pre-determined by the upper range of working conditions for the elaborated coatings. Higher values of loading and speed were selected as, for lower

**Table 1** APS deposition parameters

Powder	Particle size, $\mu\text{m}$	Arc current, A	Voltage, V	Gas flow rate, L/min			Spraying distance, mm	Coating thickness, mm
				Plasma gas		Carrier gas		
				Ar	H <sub>2</sub>	Ar		
NiAl (coatings on pins and discs)	~ 40	350-360	65	50	12-15	4	120	0.5 ± 0.05
Ni <sub>3</sub> Al (bond coat)	~ 40	350-360	65	50	12-15	4	120	0.25-0.3 ± 0.05
Organic binder								
NiAl + 15% CrB <sub>2</sub>	50-70	350-360	65	50	12-15	4	120	0.5 ± 0.05
NiAl + 30% CrB <sub>2</sub>	50-70	350-360	65	50	12-15	4	120	0.5 ± 0.05
Hot pressing								
NiAl + 15% CrB <sub>2</sub>	70-100	350-360	65	50	12-15	4	120	0.5 ± 0.05
NiAl + 30% CrB <sub>2</sub>	70-100	350-360	65	50	12-15	4	160	0.5 ± 0.05
Sintering								
NiAl + 15% CrB <sub>2</sub>	70-100	350-360	65	50	12-15	4	120	0.5 ± 0.05
NiAl + 30% CrB <sub>2</sub>	70-100	350-360	65	50	12-15	4	160	0.5 ± 0.05

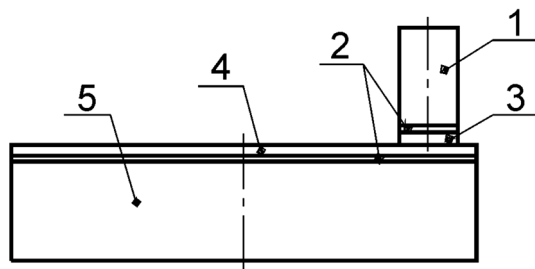


**Fig. 1** Scheme of performed wear test: 1 pin (AISI 310S), 2 bond coat (Ni<sub>3</sub>Al), 3 tested coating, 4 counter-body (NiAl coating), 5 counter-body substrate (AISI 310S)

ones, the “composite coating–intermetallic” friction pair wears at a very slow rate making any quantitative assessments inconclusive. Increasing the load beyond the planned operating range helps to intensify the process of friction and to determine the characteristic patterns of the wear mechanisms. Many works have presented the intensity of wear of composite materials and coatings using either high loads (Ref 12-15) or sliding speed (Ref 8, 16). Therefore, in this paper, a single combination of high load and speed was chosen (Table 2), as it allowed the behavior of different coatings to be compared under the same test conditions in the best way. Each test was repeated at least four times,

which helped to determine the scatter of results. Before the test, all the as-sprayed sample surfaces were mechanically ground with 150-, 180-, 500-, 800-, 1000-, 1200- and 2000-grit SiC abrasive papers. After that, the samples were polished using AMS 5/3, 3/2, 2/1, 1/0 and 0.5/0 diamond abrasive powders until their roughness ( $R_a$ ) was below 0.05  $\mu\text{m}$ , and finally cleaned with propanol. Surface roughness was measured by a Mahr MarSurf PS1 (Germany) portable surface profilometer.

The weight loss of samples during the wear test was determined by weighing them before and after the test with the use of a MettlerToledo ME204 (Switzerland) analytical balance (with a precision of 0.1 mg), which was then converted into volumetric wear. The volume loss of the pin was calculated as the volume of a conical frustum, with its height corresponding to the loss of pin material in a linear manner. This height was measured by a Mitutoyo (Japan) micrometer as the difference between the pin height before and after the test. The diameters of frustum bases were determined using a Mahr Perthometer PGK 120 (Germany) contact surface profilometer.

The coating microstructure was investigated using scanning FEI Quanta 3D (SEM) and transmission (TEM) FEI Tecnai F20 (200 kV) electron microscopes equipped with an integrated EDAX x-ray energy dispersive

**Table 2** Parameters of tribotesting

Load, N	Sliding distance, m	Sliding speed, m/s	Temperature, °C	Counter-body
150	1000	1.4	500	NiAl coating deposited on AISI 321 stainless steel disc

spectrometer (EDS). Thin foils of  $\sim 15 \mu\text{m} \times 10 \mu\text{m}$  (thickness of  $\sim 100 \text{nm}$ ) were cut out from the central part of the polished cross-section of the coatings using an FEI Quanta 200 Dual Beam FIB equipped with the Omniprobe™ lift-out system.

## Results and Discussion

### Powders and As-Deposited Coatings

Agglomerates glued with the binder were built of roughly equiaxed NiAl particles separated by channels filled with fine  $\text{CrB}_2$  particles immersed in an organic material

(Fig. 2a). The size of the agglomerates showed a bimodal distribution, with most of them having a diameter from 16 to 70  $\mu\text{m}$ , while smaller but still significant fractions were from 7 to 10  $\mu\text{m}$  (average agglomerate size  $\sim 50 \mu\text{m}$ ). The reference coating produced from these agglomerates presented a microstructure characteristic for plasma-sprayed materials, which was dominated by the presence of flattened droplets of varying contrast documenting changes in their chemical composition, similar to the  $\text{Al}_2\text{O}_3\text{-TiO}_2$  coating investigated by Sanchez et al. (Ref 17). In the present case, it consisted mostly of flattened layers of NiAl characterized by varying shades of gray, separated by occasional porosity or thin white stripes of Ni (surplus Ni in the NiAl particles is marked with dashed circles in

**Fig. 2** SEM/BSE images of microstructures of NiAl-15 wt.%  $\text{CrB}_2$  agglomerates obtained with an organic binder (a) consolidated by hot pressing (c) or sintering (e) and corresponding coatings (b, d, f) (see text for details)

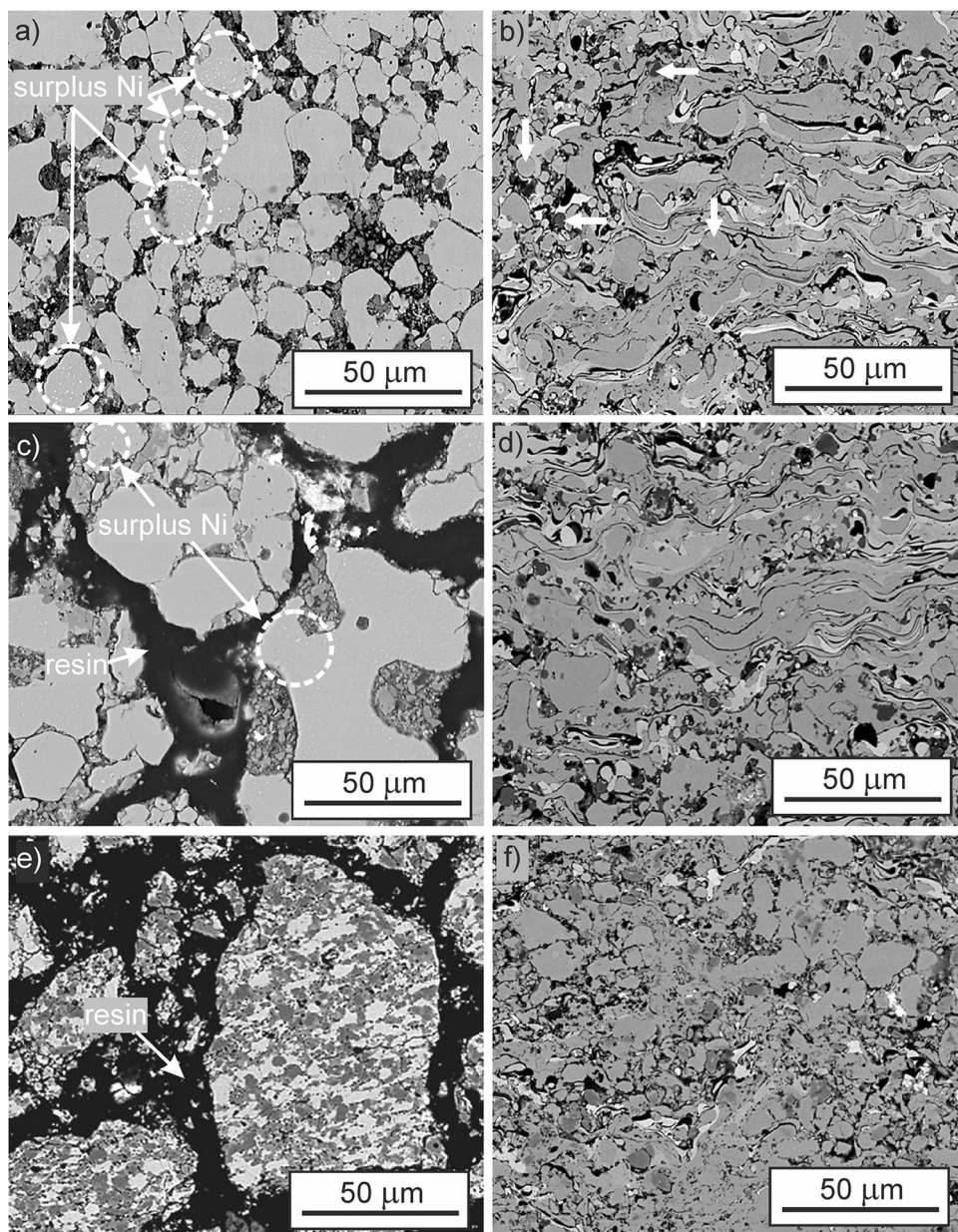


Fig. 2a, c). Simultaneously, a small number of  $\text{CrB}_2$  particles (dark gray; denoted by horizontal arrows) distributed among flattened metallic droplets could be seen (Fig. 2b). The NiAl particles, which undergo in-flight solidification, preserved their spherical shape (denoted by vertical arrows). The amount of  $\text{CrB}_2$  boride in the coating was estimated at  $\sim 8$  vol.%. It should be emphasized that the organic binder burns out instantaneously: the boride particles are disconnected from NiAl ones and have to travel by themselves. The transfer of these much finer and lighter particles to the substrate is therefore much less effective as they tend to go outside the plasma jet. Some NiAl particles also leave the stream (the plasma-spraying gun is always covered with some dust), but metal losses are much smaller (even negligible) than those of the ceramic phase.

Agglomerates obtained by hot pressing of NiAl and  $\text{CrB}_2$  powders and subsequent crushing of briquettes obtained in this way consisted of large NiAl grains (with occasionally embedded nickel particles), fused with a mixture of tightly pressed broken  $\text{CrB}_2$  borides mixed with NiAl intermetallics (Fig. 2c). The typical size of agglomerates was in the range from 70 to 100  $\mu\text{m}$ . The coating produced from this material bears a close resemblance to the previous one, i.e., it is dominated by wavy flattened droplets of varying ratios of nickel and aluminum (Fig. 2d). However, in this case, the void density is noticeably lower and dark gray particles representing  $\text{CrB}_2$  are more numerous. Additionally, in this coating, borides were located both at NiAl droplet boundaries and inside them. The performed measurements indicated that the content of  $\text{CrB}_2$  borides was up to 12 vol.%.

Agglomerates obtained from sintered NiAl and  $\text{CrB}_2$  powders are characterized by a completely different microstructure from the two previous ones, as the particles are of a composite type consisting of a NiAl matrix with interspersed fine  $\text{CrB}_2$  grains (Fig. 2e). The size of the agglomerates was the same as in the hot-pressing case. The plasma-sprayed coating (Fig. 2f) obtained from composite agglomerates showed a more refined microstructure than the two remaining coatings, i.e., those obtained using an organic binder or the hot-pressing route (Fig. 2b, d). Among others, the porosity of the former coating was lower when compared with the latter two, which is evident from the lack of larger voids. For all the composite coatings, the porosity was below 5%. Maximum porosity (4–5%) was obtained for the coating produced from powders conglomerated with the organic binder. For the coating obtained by sintering, the route porosity was within 2%. The latter coating also showed a much more uniform distribution of chromium boride particles in the matrix. The approximate amount of the latter phase was the highest of all the investigated coatings, being close to the nominal 15 vol.%.

All the above SEM observations showed that the investigated coatings bear all the features characteristic of plasma-sprayed material (Ref 18, 19), i.e., they are composed of flattened droplets of varying contrast directly referring to differences in their chemical composition, as well as occasionally being separated by pockets of oxides and voids (represented by the same dark areas). Relying on pre-alloyed powders usually helps to improve the homogenization of coatings when compared to those obtained from elemental ones (Ref 19). However, in the present coating, local contrast changes still persist. Especially characteristic in this case are thin white strands of nickel, identified in similar coatings by Tavoosi et al. (Ref 20). More importantly, the coating obtained with the sintered powder presented a more refined and less porous microstructure than those obtained from a mixture of NiAl and  $\text{CrB}_2$  through agglomeration with an organic binder or hot pressing. Additionally, the number of rounded dark gray particles representing borides is on the increase, even though their distribution is still far from homogeneous.

The STEM/TEM investigations of coatings covered both those obtained from NiAl-15 wt.%  $\text{CrB}_2$  and NiAl-30 wt.%  $\text{CrB}_2$  sintered powders. In the case of the NiAl-15 wt.%  $\text{CrB}_2$  coating, they showed the presence of up to four different types of microstructure (Fig. 3a), i.e., coarse boride crystallites with characteristic sets of parallel planar faults (Fig. 4a), smaller columnar NiAl grains nucleated at the bottoms of flattened droplets (Fig. 4b), larger NiAl crystallites with amorphous veins (Fig. 4c), and in-flight solidified spherical NiAl crystallites (Fig. 4d). The TEM/EDS measurements of local chemical compositions indicated that the veins in Fig. 4(d) bear up to  $\sim 40$  at.% Cr,  $\sim 20$  at.% Al and nickel (the rest). This is a tentative estimate as it probably carries a contribution from the surrounding matrix containing 45 at.% Al and 55 at.% Ni. The boride particles were surrounded by a layer of crystallites growing into them, securing a good connection between them and the matrix. The observations of the NiAl-30 wt.%  $\text{CrB}_2$  coatings basically confirmed the presence of the same microstructure features as in the case of lower (15 wt.%) boride addition (Fig. 3b). However, the presence of more numerous colonies of  $\text{CrB}_2$  crystallites (with characteristic planar faults; Fig. 5a) and a substitution of the amorphous channels in large parts of the NiAl matrix with fine particles dispersed in it were also noted (Fig. 5b). Locally, the matrix was filled with defects built of particle chains, which probably represent a transition stage between the amorphous channels and defect-free NiAl grains.

TEM microstructure observations confirmed that the coating with 15 wt.% addition of  $\text{CrB}_2$  contained a high density of mostly sub-micron crystallites of the latter phase. The increasing amount of  $\text{CrB}_2$  in the sintered

**Fig. 3** STEM/HAADF images of microstructure of NiAl-15 wt.% CrB<sub>2</sub> (a) and NiAl-30 wt.% CrB<sub>2</sub> coatings obtained from sintered powders

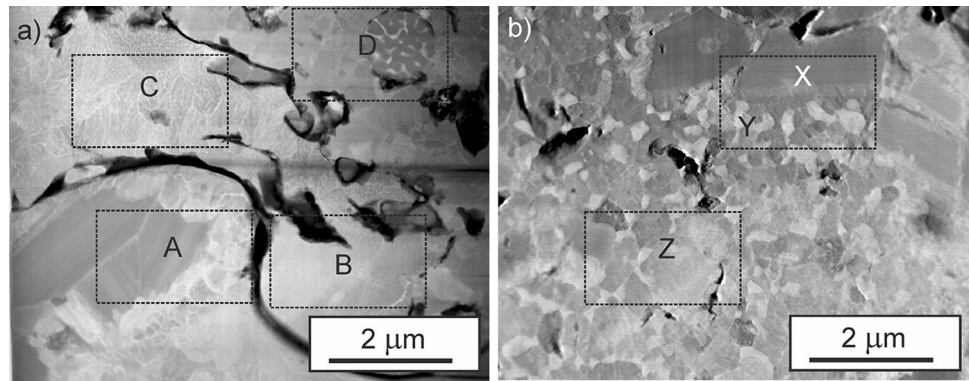


**Fig. 4** TEM/BF images of microstructure obtained from areas marked in Fig. 3(a): (a) A, (b) B, (c) C and (d) D

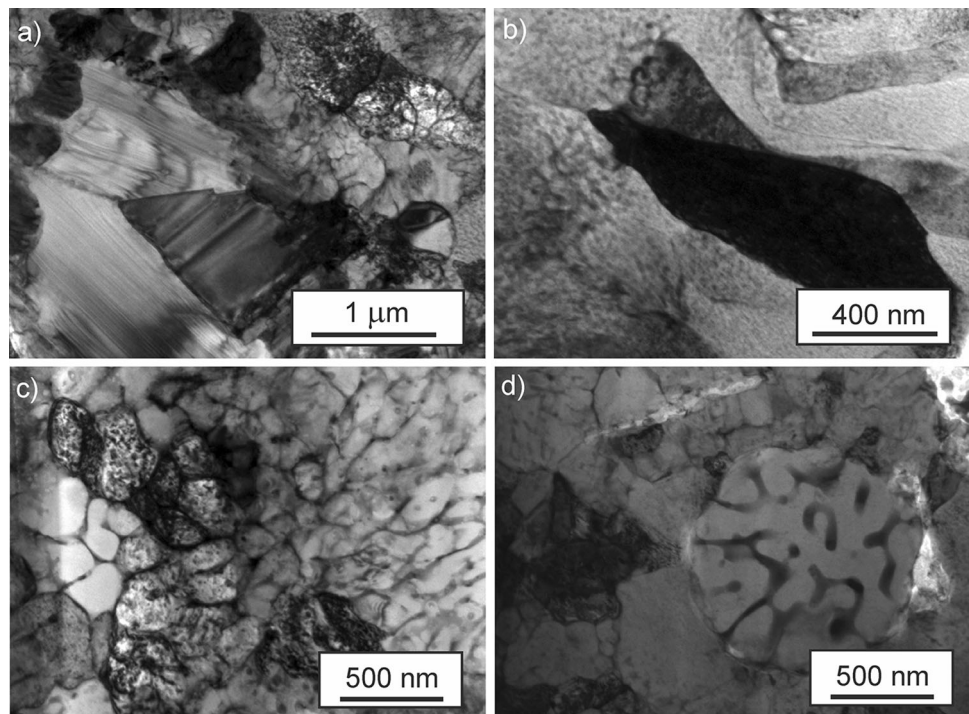
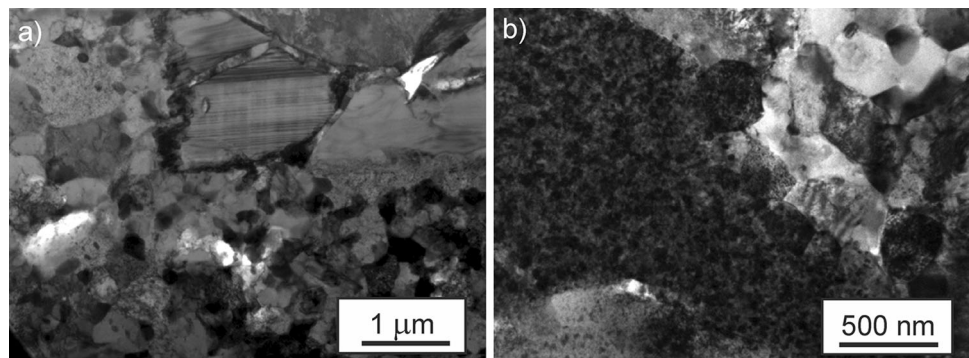


**Fig. 5** TEM/BF images of microstructure obtained from areas marked in Fig. 3(b): (a) X, Y and (b) Z



powder up to 30 wt.% resulted first of all in an even more numerous representation of these crystallites, which frequently formed small colonies. While investigating matrix/ceramic grains in a similar composite, i.e., NiAl with TiB<sub>2</sub>,

Guo et al. (Ref 21) found the presence of an oxide layer at the metal/boride interface, but none was noted in the currently investigated NiAl/CrB<sub>2</sub> interfaces. On the contrary, some of the CrB<sub>2</sub> crystallites were surrounded by chains of

crystallites growing into them. The prevailing presence of low-mass amorphous channels in the metallic matrix of both of the deposited coatings indicates that, during plasma spraying, some of the chromium boride particles also melt and dissolve in the liquid metallic droplets, only to be ejected during solidification of the NiAl phase. Unlike in some two-phase Al<sub>2</sub>O<sub>3</sub>-TiO<sub>2</sub> plasma-sprayed coatings, where larger pockets of starting powders were embedded among the flattened droplets of a mixture of these oxides (Ref 17), all the current materials show signs of being melted and solidified either in-flight or on hitting the substrate.

**Wear Test**

The developed materials are intended to operate as high-temperature friction units, and therefore wear tests of coatings were conducted under dry sliding friction conditions at their anticipated working temperature range, i.e., at 500 °C (Tables 2, 3 and Fig. 6).

The friction coefficient for the reference NiAl coating was within the 0.43-0.48 range, while, for NiAl with 15 and 30 wt.% CrB<sub>2</sub> produced with an organic binder, it was lowered to 0.35-0.36 and 0.37-0.39, respectively. The coatings obtained using the same amounts of boride but produced using the hot pressing or sintering routes also gave relatively low friction values of 0.27-0.3 and 0.26-0.29, respectively, for 15 wt.% CrB<sub>2</sub> and only slightly higher (0.31-0.33) for 30 wt.% CrB<sub>2</sub>. The above results clearly show that even an admixture of chromium boride into the NiAl powders lowers the friction of the plasma-sprayed coatings, though the smaller applied addition is more effective in this role.

According to the results (Table 3 and Fig. 6), the “NiAl coating–NiAl coating” friction pair undergoes the highest wear. Among others, this is due to some softening of this intermetallic during friction at elevated temperatures. A

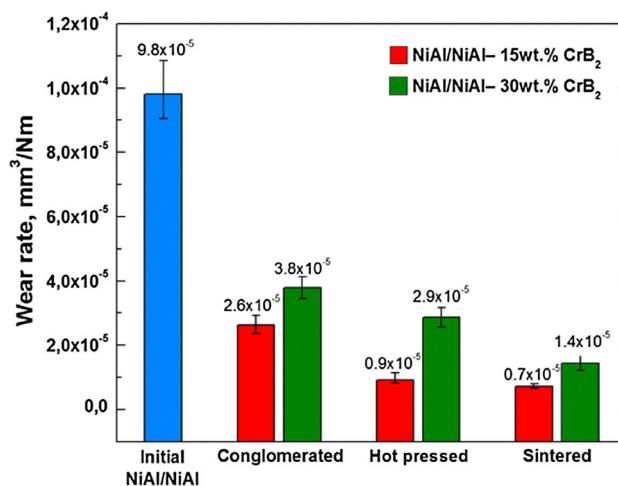


**Fig. 6** Wear rate of plasma-sprayed NiAl-CrB<sub>2</sub> composite coatings obtained by various routes

detailed wear mechanism of such a friction pair and the wear of composite coatings conglomerated on an organic binder has been documented elsewhere (Ref 9-11).

The admixture of CrB<sub>2</sub> into NiAl powders helped to lower the wear rate of the plasma-sprayed coatings obtained from all the types of agglomerated powders used in the present experiment. Namely, the wear intensity of the friction pair with NiAl/NiAl-15 wt.% CrB<sub>2</sub> coatings produced with an organic binder, hot pressing and sintering were lowered to 2.6, 0.9 and 0.7 mm<sup>3</sup>/Nm 10<sup>-5</sup>, respectively (Fig. 6). The coatings with the CrB<sub>2</sub> addition increased to 30 wt.% also showed better wear resistance when compared with the reference one, even though the measured values were evidently higher in all cases, i.e., the wear rate changed to 3.8, 2.9 and, finally, to 1.4 mm<sup>3</sup>/Nm 10<sup>-5</sup> for those agglomerated with an organic binder, hot pressed and sintered, respectively. All these results confirmed the strong influence of powder preparation on the capability of the coating to withstand loading at work.

**Table 3** Results of wear tests

Number of tests	Wear rate of friction pair (mm <sup>3</sup> /Nm 10 <sup>-5</sup> )						
	Initial NiAl/NiAl friction pair	Materials					
		NiAl/NiAl-15 wt.% CrB <sub>2</sub>			NiAl/NiAl-30 wt.% CrB <sub>2</sub>		
		Conglomerated on organic binder	Hot pressed	Sintered	Conglomerated on organic binder	Hot pressed	Sintered
1	9.29	2.93	1.14	0.79	3.66	3.17	1.44
2	9.86	2.37	0.81	0.69	4.05	3.05	1.70
3	10.86	2.75	0.91	0.67	3.47	2.56	1.21
4	9.05	2.52	1.06	0.74	4.13	2.97	1.62
Average	9.81	2.62	0.91	0.72	3.79	2.88	1.44

SEM observations of wear track morphology revealed that all the samples were pock-marked with voids left by broken-out particles. These voids were more numerous in coatings obtained from hot-pressed powders than those deposited using sintered ones (Fig. 7). The former with the higher 30 wt.% CrB<sub>2</sub> addition were also characterized by larger cavities lined at their edges with colonies of boride powder particles (dashed circles in Fig. 7b). The wear track of the coating obtained using the sintered powder with 15 wt.% CrB<sub>2</sub> showed the smoothest surface of all the investigated specimens. In that case, both NiAl (light gray spherical, marked with arrows) and CrB<sub>2</sub> particles (dark gray with a rounded or irregular shape, marked with double arrows) were abraded, but stayed embedded (Fig. 7c).

The lowest wear intensity of all the investigated coatings was in the one characterized by the most refined microstructure, i.e., that obtained from sintered NiAl and CrB<sub>2</sub> powders. It was roughly 20 times smaller than that measured for coatings obtained just from NiAl powders (Ref 10), and still 4 times less than for the coatings deposited using the same mixture of initial powders but agglomerated with an organic binder. The above improvement in wear-resistance results, not only from microstructure refinement but also from the reaction of CrB<sub>2</sub> and the NiAl matrix, is proved by the TEM observations. The first one helps to cancel crack propagation,

while the second allows a better connection between the chromium borides and the matrix to be obtained. The particles, which are hard and well-fused with the metallic matrix, are more efficient in dissipating the external load within the coating. The higher wear documented for coatings with 30 than those with 15 wt.% CrB<sub>2</sub> obtained for all of the applied processing routes was found to be a result of the formation of boride colonies. Under mechanical loading, the boundaries of such colonies open an easy way for crack propagation, causing the removal of larger chunks of material from the coating surface.

Additional studies of the intermetallic counter-body surface after wear tests showed that the NiAl/NiAl-30 wt.% CrB<sub>2</sub> friction pair (Fig. 8b, d) is characterized by the presence of deeper grooves and wider areas of damage when compared with NiAl/NiAl-15 wt.% CrB<sub>2</sub> (Fig. 8a, c). This is explained by the fact that an increased content of the refractory component leads to embrittlement of the coating and local chipping of individual boride grains. Such grains will act as an abrasive material in tribological tests. On the friction surface, one may observe the presence of fracture sites in the form of pits (Fig. 8b), explaining their higher wear values (Fig. 6). On the other hand, on the counter-body surface of the NiAl/NiAl-15 wt.% CrB<sub>2</sub> friction pair (Fig. 8a, c), only the presence of separate,

**Fig. 7** SEM/BSE images of worn surfaces of NiAl-15 wt.% CrB<sub>2</sub> (a, c) and NiAl-30 wt.% CrB<sub>2</sub> (b, d) plasma coating after tribo-tests at 500 °C; obtained from hot-pressed powders (a, b) and sintered (c, d)

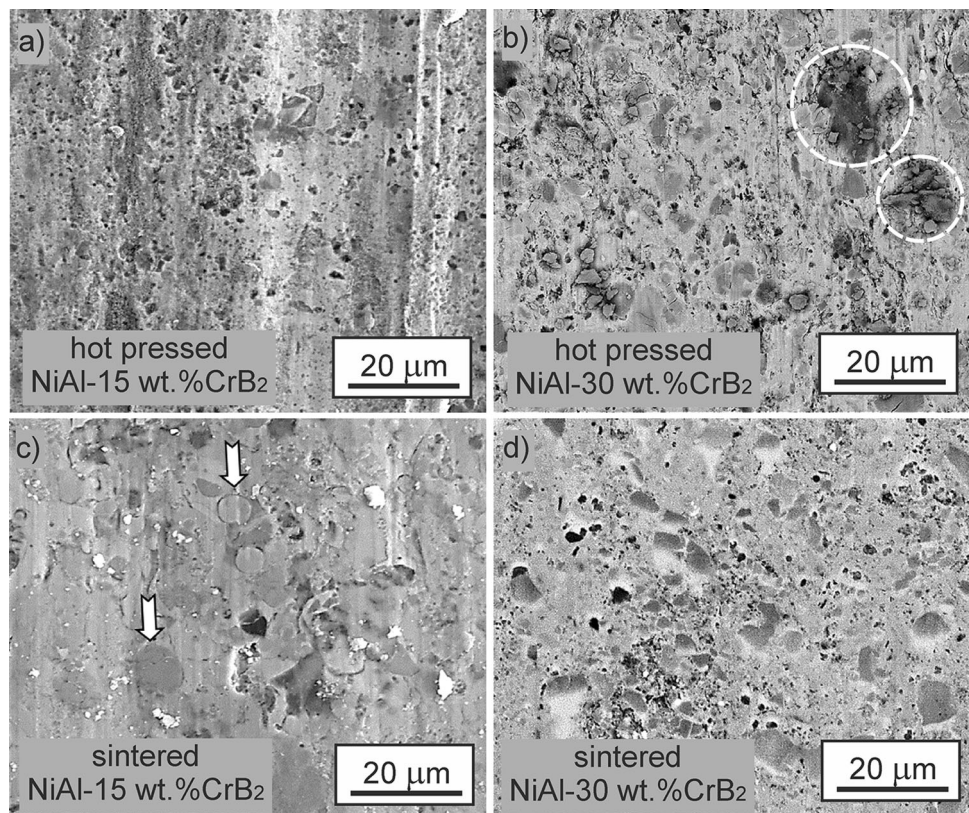
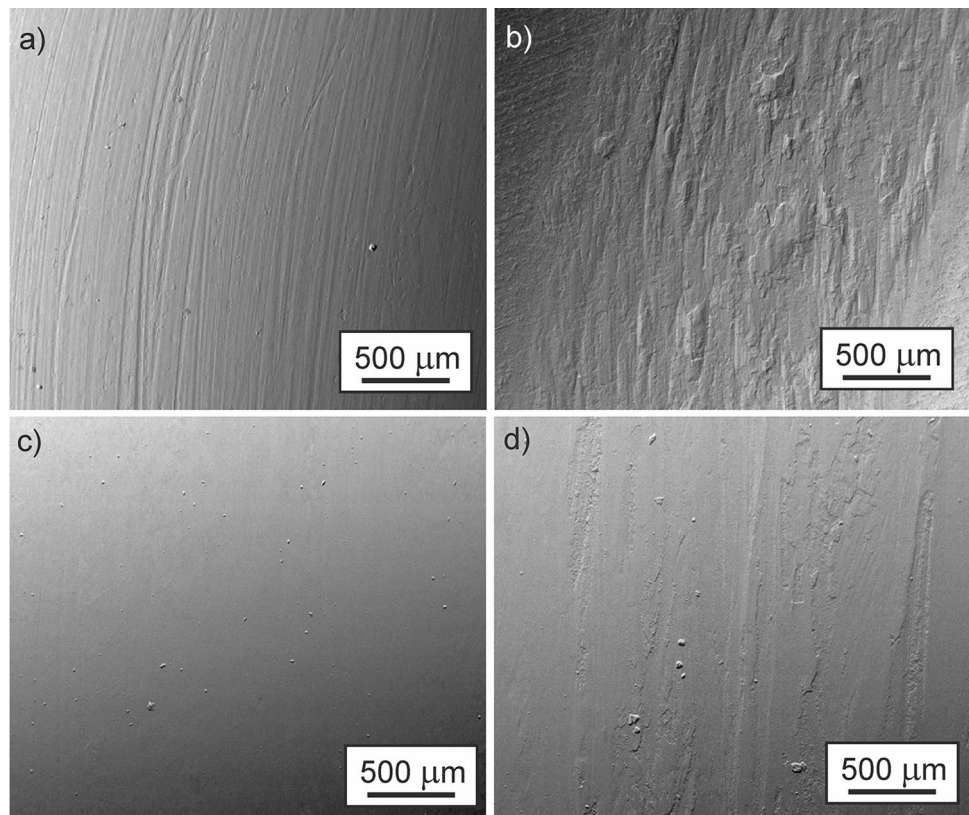


**Fig. 8** SEM images of NiAl plasma coating (disc) worn surfaces after tribo-tests at 500 °C in pairs with NiAl-15 wt.% CrB<sub>2</sub> (a, c) and NiAl-30 wt.% CrB<sub>2</sub> (b, d) plasma coating; obtained from hot-pressed powders (a, b) and sintered ones (c, d)



quite thin, grooves could be differentiated (the absence of any otherwise damaged areas is notable).

## Summary and Conclusions

The SEM and TEM observations of NiAl and CrB<sub>2</sub> agglomerates used for atmospheric plasma deposition, as well as the NiAl/CrB<sub>2</sub> coatings, helped to explain that the improvement in wear resistance of such composite deposits results partly from their microstructure refinement and partly from the good connection between chromium boride and the NiAl matrix. The performed experiments helped to establish that:

1. The presence of amorphous channels rich in Cr within the NiAl matrix of the NiAl/CrB<sub>2</sub> coatings is a clear indication of in-flight melting and mutual dissolution of intermetallic and some boride particles, followed by segregation during their subsequent solidification.
2. The formation of rims of crystallites growing into boride particles remaining solid throughout the plasma spray deposition process directly confirms the strong reactivity between liquid NiAl and solid CrB<sub>2</sub>, indicating the presence of good wetting in this system.
3. The better microstructure refinement of agglomerates prepared through sintering, i.e., with liquid NiAl when

compared with that obtained through an organic binder or hot pressing—both of the latter achieved through a solid state path—has to be the result of a good wetting of chromium boride by the NiAl intermetallic.

4. An increasing amount of CrB<sub>2</sub> from 15 to 30 wt.% increases the wear rate of these coatings, because larger additions of boride phase in plasma-sprayed material show a tendency to form colonies of ceramic particles (from the fraction remaining solid during plasma spraying), which is a weak link during their loading.
5. The sintering route for preparing composite agglomerates prevented any significant losses of boride phase during plasma spraying, which made this method the most effective, as it concerns a nominal boride content being obtained in the NiAl/CrB<sub>2</sub> coatings.

Taking all the above into account, the best wear resistance was obtained for the friction pair with the NiAl/NiAl-15 wt.% CrB<sub>2</sub> coating obtained with sintered powder. However, the effect of a well-represented amorphous channel sub-structure in the NiAl matrix on the wear process requires further study. This and the eventual role of oxidizing processes of the worn surface can only be answered by detailed investigation of the phase and chemical composition of the wear debris.

**Acknowledgments** This work was supported by the Grant for monthly research in Poland according to the Protocol to the Agreement on Scientific Cooperation between the National Academy of Sciences of Ukraine and Polish Academy of Sciences (being part of statutory activity of the latter). Special thanks to the Tallinn University of Technology and to Dr. Maksim Antonov for the help in carrying out of wear tests.

**Open Access** This article is distributed under the terms of the Creative Commons Attribution 4.0 International License (<http://creativecommons.org/licenses/by/4.0/>), which permits unrestricted use, distribution, and reproduction in any medium, provided you give appropriate credit to the original author(s) and the source, provide a link to the Creative Commons license, and indicate if changes were made.

## References

1. D.B. Miracle and R. Darolia, NiAl and Its Alloys, *Structural Applications of Intermetallic Compounds*, J.H. Westbrook and R.L. Fleischer, Eds., Wiley, New York, 2000, p 20
2. R. Darolia, NiAl Alloys for High Temperature Structural Applications, *JOM*, 1991, **43**, p 44-48
3. S. Zhu, Q. Bi, M. Niu, J. Yang, and W. Liu, Tribological Behavior of NiAl Matrix Composites with Addition of Oxides at High Temperatures, *Wear*, 2012, **274-275**, p 423-434
4. J.D. Whittenberger, R.K. Viswanadham, S.K. Mannan, and B. Sprissler, Elevated Temperature Slow Plastic Deformation of NiAl-TiB<sub>2</sub> Particulate Composites at 1200 and 1300 K, *J. Mater. Sci.*, 1990, **25**, p 35-44
5. J.D. Whittenberger, S. Kumar, S.K. Mannan, and R.K. Viswanadham, Slow Plastic Deformation of Extruded NiAl-10TiB<sub>2</sub> Particulate Composites at 1200 and 1300 K, *J. Mater. Sci. Lett.*, 1990, **9**, p 326-328
6. B. Movahedi, Fracture Toughness and Wear Behavior of NiAl-Based Nanocomposite HVOF Coatings, *Surf. Coat. Technol.*, 2013, **235**, p 212-219
7. A.A. Shokati, N. Parvin, N. Sabzianpour, M. Shokati, and A. Hemmati, In Situ Synthesis of NiAl-NbB<sub>2</sub> Composite Powder Through Combustion Synthesis, *J. Alloys Compd.*, 2013, **549**, p 141-146
8. L.Y. Sheng, F. Yang, T.F. Xi, and J.T. Guo, Investigation on Microstructure and Wear Behavior of the NiAl-TiC-Al<sub>2</sub>O<sub>3</sub> Composite Fabricated by Self-Propagation High-Temperature Synthesis with Extrusion, *J. Alloys Compd.*, 2013, **554**, p 182-188
9. O. Umanskyi, O. Poliarus, M. Ukrainets, and I. Martsenyuk, Effect of ZrB<sub>2</sub>, CrB<sub>2</sub> and TiB<sub>2</sub> Additives on the Tribological Characteristics of NiAl-Based Gas-Thermal Coatings, *Key Eng. Mater.*, 2014, **604**, p 20-23
10. A.P. Umanskii, E.N. Polyarus, M.S. Ukrainets, and L.M. Kapitanchuk, Structure and Tribotechnical Characteristics of NiAl-CrB<sub>2</sub> Composite Materials and Coatings, *Powder Metall. Met. Ceram.*, 2015, **54**, p 1-2
11. O. Umanskyi, O.M. Poliarus, M. Ukrainets, and M. Antonov, Physical-Chemical Interaction in NiAl-MeB<sub>2</sub> Systems Intended for Tribological Applications, *Weld. J.*, 2015, **94**, p 225-230
12. P. Xia, G. Han, and K. Xie, Effect of Compositions on the Microstructure and Properties of Plasma Clad NiAl Coating, *Met. Mater. Int.*, 2016, **22**, p 424-429
13. L. Fu, W. Han, L. Zhao, K. Gong, S. Bengtsson, M. Zhou, C. Li, and Z. Tian, Effects of Cr<sub>3</sub>C<sub>2</sub> Content and Temperature on Sliding Friction and Wear Behaviors of Cr<sub>3</sub>C<sub>2</sub>/Ni<sub>3</sub>Al Composite Materials, *Wear*, 2018, **414-415**, p 163-173
14. Y. Chen and H.M. Wang, Microstructure and Wear Resistance of Laser-Melted TiC Reinforced Nickel Aluminide Dual-Phase Matrix In Situ Composite, *Intermetallics*, 2006, **14**, p 325-331
15. K. Gong, H. Luo, D. Feng, and C. Li, Wear of Ni<sub>3</sub>Al-Based Materials and Its Chromium-Carbide Reinforced Composites, *Wear*, 2008, **265**, p 1751-1755
16. J. Cheng, F. Li, S. Zhu, J. Hao, J. Yang, W. Li, and W. Liu, High Temperature Tribological Properties of a Nickel-Alloy-Based Solid Lubricating Composite: Effect of Surface Tribo-Chemistry, Counterpart and Mechanical Properties, *Wear*, 2017, **386-387**, p 39-48
17. E. Sanchez, E. Bannier, V. Cantavella, M.D. Salvador, E. Klyatskina, J. Morgiel, J. Grzonka, and A.R. Boccaccini, Deposition of Al<sub>2</sub>O<sub>3</sub>-TiO<sub>2</sub> Nano-Structured Powders by Atmospheric Plasma Spraying, *J. Therm. Spray Technol.*, 2008, **17**, p 329-337
18. S. Deshpande, T.S. Sampath, and H. Zhang, Mechanisms of Oxidation and Its Role in Microstructural Evolution of Metallic Thermal Spray Coatings—Case Study for Ni-Al, *Surf. Coat. Technol.*, 2006, **200**, p 5395-5406
19. K. Izdinsky, J. Dufek, J. Ivan, M. Zemankova, P. Minar, and Z. Izdinska, Microstructure of Air Plasma-Sprayed NiAl Coating, *Kov. Mater.*, 2003, **41**, p 365-376
20. M. Tavoosi, H. Heydari, A. Hosseinkhani, and B. Adelimoghaddam, Effects of Crystalline Growth on Corrosion Behaviour of Nanocrystalline NiAl Coating, *Bull. Mater. Sci.*, 2015, **38**, p 895-899
21. J.T. Guo, D.T. Jiang, Z.P. Xing, and G.S. Lia, Tensile Properties and Microstructures of NiAl-20TiB and NiAl-20TiC In Situ Composites, *Mater. Des.*, 1997, **18**, p 357-360

**Publisher's Note** Springer Nature remains neutral with regard to jurisdictional claims in published maps and institutional affiliations.